Lysosomal degradation products induce *Coxiella burnetii* virulence

Patrice Newton[a], David R. Thomas[a], Shawna C. O. Reed[b,1], Nicole Lau[a], Bangyan Xu[c], Sze Ying Ong[d], Shivani Pasricha[d], Piyush B. Madhamshettiwar[e], Laura E. Edgington-Mitchell[f,g], Kaylene J. Simpson[e,h], Craig R. Roy[b], and Hayley J. Newton[a,2]

[a]Department of Microbiology and Immunology, Peter Doherty Institute for Infection and Immunity, The University of Melbourne, Melbourne, VIC 3000, Australia; [b]Department of Microbial Pathogenesis, Boyer Center for Molecular Medicine, Yale University School of Medicine, New Haven CT 06510; [c]Department of Biochemistry and Molecular Biology, Bio21 Molecular Science and Biotechnology Institute, The University of Melbourne, Parkville, VIC 3052, Australia; [d]Centre for Innate Immunity and Infectious Diseases, Hudson Institute of Medical Research, Clayton, VIC 3168 Australia; [e]Victorian Centre for Functional Genomics, Peter MacCallum Cancer Centre, Melbourne, VIC 3000, Australia; [f]Drug Discovery Biology, Monash Institute of Pharmaceutical Sciences, Monash University, Parkville, VIC 3052, Australia; [g]Department of Oral and Maxillofacial Surgery, Bluestone Center for Clinical Research, New York University College of Dentistry, New York, NY 10010; and [h]Sir Peter MacCallum Department of Oncology, University of Melbourne, Parkville, VIC 3010, Australia

Edited by Philippe J. Sansonetti, Institut Pasteur, Paris, France, and approved February 13, 2020 (received for review December 9, 2019)

***Coxiella burnetii* is an intracellular pathogen that replicates in a lysosome-like vacuole through activation of a Dot/Icm-type IVB secretion system and subsequent translocation of effectors that remodel the host cell. Here a genome-wide small interfering RNA screen and reporter assay were used to identify host proteins required for Dot/Icm effector translocation. Significant, and independently validated, hits demonstrated the importance of multiple protein families required for endocytic trafficking of the *C. burnetii*-containing vacuole to the lysosome. Further analysis demonstrated that the degradative activity of the lysosome created by proteases, such as TPP1, which are transported to the lysosome by receptors, such as M6PR and LRP1, are critical for *C. burnetii* virulence. Indeed, the *C. burnetii* PmrA/B regulon, responsible for transcriptional up-regulation of genes encoding the Dot/Icm apparatus and a subset of effectors, induced expression of a virulence-associated transcriptome in response to degradative products of the lysosome. Luciferase reporter strains, and subsequent RNA-sequencing analysis, demonstrated that particular amino acids activate the *C. burnetii* PmrA/B two-component system. This study has further enhanced our understanding of *C. burnetii* pathogenesis, the host–pathogen interactions that contribute to bacterial virulence, and the different environmental triggers pathogens can sense to facilitate virulence.**

Coxiella burnetii | Dot/Icm secretion system | virulence regulation | siRNA screen | amino acid sensing

Coxiella burnetii, the causative agent of human Q fever, is an important zoonotic pathogen. Inhalation of contaminated aerosols, commonly through exposure to infected animals, can cause an acute systemic infection frequently involving pneumonia or hepatitis (1). A small proportion of infected individuals will develop persistent chronic Q fever with life-threatening complications such as endocarditis.

Following inhalation, the bacteria infect alveolar macrophages and replicate to high numbers within these cells (2, 3). The intracellular niche of *C. burnetii* is a unique, spacious vacuole termed the *Coxiella*-containing vacuole (CCV). The *C. burnetii*-containing phagosome undergoes endocytic trafficking to mature into the normally bactericidal lysosome where conditions stimulate *C. burnetii* metabolism and biogenesis of the CCV (4). The CCV retains the low pH and hydrolytic features of a lysosome but is also modified by the pathogen to facilitate replication. Key features of the mature CCV include significant expansion, through interaction with intracellular vesicles including autophagosomes, clathrin-coated vesicles, and endocytic vesicles, and a strong antiapoptotic influence on the host cell (5, 6).

Recently, the development of methods to axenically cultivate and genetically manipulate *C. burnetii* has led to a revolution in the capacity to explore the molecular details of the host–pathogen interactions mediated by *C. burnetii* (7–9). Multiple mutagenesis studies have confirmed that intracellular replication of *C. burnetii*, and therefore virulence, requires a functional Dot/Icm-type IVB secretion system (10–14). This specialized secretion apparatus allows the pathogen to introduce a large repertoire of effector proteins into the host cytosol. Although the biochemical functions of individual effectors are poorly understood, it is clear that these effectors work in concert to manipulate host cell processes and create the replicative niche while still maintaining host cell homeostasis (5).

The *C. burnetii* Dot/Icm system is functionally analogous to the well-studied Dot/Icm system of *Legionella* species, which is essential for intracellular replication of Legionnaires' disease-causing pathogens (15). Despite depending on the same apparatus for virulence, the replicative niches of *Legionella* and *C. burnetii* are quite divergent. *Legionella* species actively evade the endocytic pathway, with the *Legionella*-containing vacuole (LCV) acquiring markers of the endoplasmic reticulum and secretory pathway rapidly following phagocytosis (16). The distinct vacuolar destinations of these closely related pathogens are mediated by the unique

Significance

***Coxiella burnetii* is a unique bacterial pathogen that replicates to high numbers in a lysosome-like intracellular niche. This study identified host proteins that contribute to the pathogen's capacity to establish this niche and activate the Dot/Icm secretion system required for intracellular replication. Many host proteins were found to contribute to the establishment of *C. burnetii* virulence by aiding trafficking of the pathogen to the lysosome and creating the degradative lysosome environment. Pathogenic bacteria are able to sense and adapt to their environment by altering their gene expression profile. Here we demonstrated that *C. burnetii* detects specific amino acids present in the lysosome using a two-component system that up-regulates expression of genes required for Dot/Icm activity.**

Author contributions: P.N., S.C.O.R., S.Y.O., L.E.E.-M., K.J.S., C.R.R., and H.J.N. designed research; P.N., D.R.T., S.C.O.R., N.L., B.X., and H.J.N. performed research; P.N., D.R.T., K.J.S., and H.J.N. contributed new reagents/analytic tools; P.N., S.C.O.R., N.L., S.P., P.B.M., and H.J.N. analyzed data; and P.N. and H.J.N. wrote the paper.

The authors declare no competing interest.

This article is a PNAS Direct Submission.

[1]Present address: Department of Biomedical Sciences, Quinnipiac University, Hamden, CT 06518.

[2]To whom correspondence may be addressed. Email: hnewton@unimelb.edu.au.

This article contains supporting information online at https://www.pnas.org/lookup/suppl/doi:10.1073/pnas.1921344117/-/DCSupplemental.

First published March 9, 2020.

repertoires of Dot/Icm effectors and the exquisite control each pathogen has over Dot/Icm activation. The *Legionella* Dot/Icm system must be active immediately upon contact with a eukaryotic cell to prevent endocytic maturation of the LCV. Indeed, *Legionella pneumophila* effector translocation occurs upon intimate contact with the host plasma membrane even when entry is blocked (17). In contrast, *C. burnetii* effector translocation is delayed until the pathogen reaches the acidic confines of the lysosome (18). Silencing expression of endocytic Rab GTPases Rab5 or Rab7 or chemically disrupting lysosome acidification with the vacuolar ATPase inhibitor Bafilomycin A leads to a significant reduction in *C. burnetii* effector translocation (18, 19). This has been demonstrated using a reporter assay where *C. burnetii* has been engineered to constitutively express β-lactamase (BlaM) transcriptionally fused to an effector and BlaM activity in the host cytosol is measured as a proxy for effector translocation (19). Expression of Dot/Icm apparatus genes and a cohort of Dot/Icm effectors is controlled by the PmrA/B two-component regulatory system in both *C. burnetii* and *L. pneumophila* (20, 21). This system is essential for *C. burnetii* intracellular replication, indicating that transcriptional control is integral to Dot/Icm activation (13, 14, 21).

Here the robust β-lactamase reporter assay and delayed effector translocation by *C. burnetii* have been harnessed as a tool to define human host factors that contribute to both bacterial transport to a lysosome in general and the specific environmental conditions within the lysosome that signal *C. burnetii*, through PmrA/B, to trigger virulence. This study has significantly advanced understanding of *C. burnetii* pathogenesis and the importance of various host systems in developing its intracellular niche.

Results

Genome-Wide Small Interfering RNA Screen of Host Genes Necessary for Efficient *C. burnetii* Dot/Icm Effector Translocation. Previous work established the importance of the host endocytic pathway for efficient effector translocation by *C. burnetii* (18, 22). To globally elucidate the host genes required for *C. burnetii* effector translocation, and therefore virulence, a high-throughput genome-wide small interfering RNA (siRNA) screen was performed (Fig. 1*A*). Effector translocation was examined using a reporter *C. burnetii* Nine Mile phase II (NMII) strain constitutively expressing the known effector protein MceA (10, 23) with an N-terminal BlaM fusion and the fluorescent BlaM substrate CCF2-AM. Following excitation at 410 nm, cleavage of CCF2-AM by BlaM leads to a shift in fluorescence emission from 520 nm (green) to 450 nm (blue). The 450:520-nm ratio was used to assess BlaM–MceA translocation into the host cytosol.

HeLa cells were transfected with an siRNA SMARTpool library targeting 18,120 individual protein-coding genes in a 96-well plate-arrayed format for 72 h and then infected with *C. burnetii* NMII pBlaM–MceA. Effector translocation was measured 24 h postinfection using the fluorescent substrate CCF2-AM prior to fixation and high-content imaging quantification of cell viability within individual wells using the nuclear stain DRAQ5. Controls were used on each 96-well plate to assess transfection efficiency and assay robustness. Both mock-transfected cells, delivered lipid but no siRNA, and ON-TARGET plus-nontargeting control (siOTP-NT) SMARTpool were used as negative controls (24). Cells transfected with the siRab7A SMARTpool were used as a positive control for the reduction of effector translocation, and cells transfected with the siPLK1 (polo-like kinase 1) SMARTpool were used as a transfection control since depletion of PLK1 results in cell death (25).

The standard hit-identification approach for siRNA screens is the application of a robust *Z*-score normalization across all screen plates (26, 27). *Z*-score normalization to siOTP-NT revealed 82 and 968 genes for which the translocation ratio was significantly decreased or increased, respectively (Dataset S1). The decrease in translocation ratio observed within the 82 genes ranged from 76 to 62% compared with siOTP-NT. The average translocation ratio reduction across all screened plates for the siRab7A SMARTpool

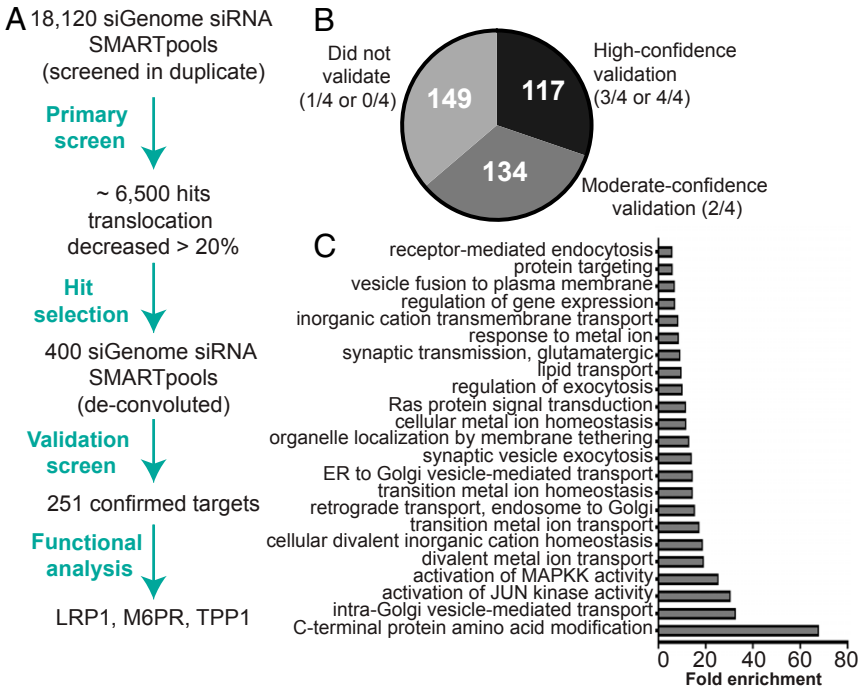

Fig. 1. Genome-wide siRNA screen of host genes necessary for efficient *C. burnetii* Dot/Icm effector translocation. (*A*) Summary of the overall siRNA screen including hit selection and confirmed targets. (*B*) Pie chart displaying the overall outcome from the deconvoluted validation screen of the selected 400 targets. (*C*) Enrichment analysis of the biological process categories that were overrepresented in the 251 validated targets using the PANTHER overrepresentation test against the *Homo sapiens* genome reference list.

control was 56.5 ± 7.5% compared with siOTP-NT. Since the focus of this study was the identification of host proteins that adversely affected effector translocation, the majority of the 400 genes selected for the secondary validation screen demonstrated at least a 25% reduction in translocation relative to siOTP-NT. Included in this cohort were 53 out of the possible 82 genes that had demonstrated a statistically significant decrease in translocation (Dataset S2). The impact of individual siRNA treatment on cell viability was also considered during target selection for the secondary screen. More than 50% cell viability was considered acceptable. Since the assay readout is ratiometric, results were minimally affected by changing cell numbers. Targets with >50% toxicity following the secondary screen were not considered for any follow-up analysis.

The validation screen of 400 selected targets was performed using the same assay format as the primary screen; however, the siRNA SMARTpools were deconvoluted and the four individual duplex siRNAs were screened separately. Defining the level of confidence in validation of selected targets was determined by approximate reproduction of the translocation ratio observed during the primary screen and a minimum decrease in effector translocation of 20% compared with siOTP-NT (Fig. 1*B* and Dataset S3). Using this classification, 117 genes validated with high confidence (3/4 or 4/4 siRNAs), 134 genes with moderate confidence (2/4 siRNAs), and 149 genes did not validate (1/4 or 0/4 siRNAs) (Dataset S3). Enrichment analysis of the validated 251 using the PANTHER classification system (28) revealed biological process categories that were statistically overrepresented (Fig. 1*C* and *SI Appendix*, Table S1).

Genome-Wide Screen Validates the Importance of the Host Endocytic Trafficking Pathway for *C. burnetii* Infection. This screen demonstrated that host proteins involved in the endocytic pathway, including the Rab and SNARE (soluble NSF attachment protein receptor) protein families and vacuolar protein-sorting (VPS) proteins, are required for efficient effector translocation by *C. burnetii*. Validated targets included key regulators of membrane transport (including RAB5A and RAB7A) and the Rab protein modifier RABGGTA (29, 30). The strongest hit from the primary screen, NAPA (alpha-soluble NSF attachment protein, also known as SNAP-α), validated with high confidence together with NAPB (beta-soluble NSF attachment protein; SNAP-β) and NSF (*N*-ethylmaleimide–sensitive factor), which act together to manipulate SNARE proteins during vesicle-mediated transport (31–33). Components of the eukaryotic retromer complex also validated strongly, including those of the core complex (VPS29 and VPS35) and the cargo adapters, also known as sorting nexins (SNX1, SNX3, and SNX6) (34, 35). These components were previously identified in the siRNA screen by McDonough et al. (22), who investigated the impact of silencing gene expression of host proteins on *C. burnetii* replication. Our data confirm that the retromer complex plays an important role in establishment of *C. burnetii* infection. Proteins involved in the ESCRT (endosomal sorting complexes required for transport) complexes were important, including VPS4B and VPS25 (36, 37), and SNARE proteins whose functions have not been fully elucidated were also identified, such as SNX22 and SNX24, suggesting a potential role for these proteins in endocytic trafficking.

In addition to a requirement for endocytic trafficking, *C. burnetii* also exploits the eukaryotic autophagy pathway to establish its replicative niche (38, 39). The importance of this host pathway was confirmed in the primary screen since a third of the known autophagy family members (11 out of 33) produced an observable translocation defect when silenced (Dataset S1). Five of these members were further examined in the validation screen, of which three were validated (ATG4B and ATG5 [moderate confidence] and ATG12 [high confidence]; Dataset S3). The identification of two members of the Atg5–Atg12–Atg16 complex, which has an integral role in the autophagic process within the host (40), highlights the importance of autophagy during establishment of *C. burnetii* infection.

Lysosomal Proteins Are Necessary for Efficient Effector Translocation by *C. burnetii*. The *C. burnetii* replicative niche is a bacterially modified lysosome that maintains an acidic pH and the presence of lysosomal enzymes and membrane proteins (41, 42). Given this lysosomal niche, primary screen results for proteins previously confirmed as resident lysosomal proteins (43) were analyzed (*SI Appendix*, Table S2). Of the 184 lysosomal proteins assessed, silencing of 72 led to a decrease in effector translocation of at least 20% compared with siOTP-NT–treated cells, demonstrating the significance of the lysosomal environment in triggering *C. burnetii* virulence.

A subset of 23 lysosomal targets were tested in the validation screen, of which 13 validated with either high or moderate confidence (*SI Appendix*, Table S2). These included vacuolar ATPase subunits (ATP6V0C and ATP6V1E1) responsible for acidification of the lysosome (44), and several lysosomal enzymes, including the hydrolases cathepsin B (CTSB) and cathepsin C (CTSC), sialidase-1 (NEU1), and beta-mannosidase (MANBA). Additionally, lysosomal transporters confirmed in the validation screen to be important for bacterial effector translocation included the cholesterol transporters Niemann–Pick C1 (NPC1) and Niemann–Pick C2 (NPC2), a sodium-independent sulfate anion transporter (SLC26A11), and the lysosomal cysteine transporter cystinosin (CTNS).

Given that gene silencing of so many lysosomal proteins led to reduced Dot/Icm protein translocation, the ability of the cell to deliver these proteins to the lysosome should also be required. The majority of these proteins acquire mannose-6-phosphate (Man-6-P) moieties that are recognized by either cation-dependent or cation-independent Man-6-P receptors (M6PRs) enabling transport to the lysosome (45), although several alternative receptors that enable the sorting of lysosomal enzymes independent of Man-6-P have also been identified (46). Thus, the dependence of effector translocation on a subset of recognized lysosomal trafficking receptors identified in the primary siRNA screen was investigated further (Fig. 2*A*). A decrease in effector translocation was consistently observed for low-density lipoprotein receptor-related protein 1 (LRP1) and cation-dependent M6PR (Fig. 2*A*). Simultaneous depletion of *LRP1* and *M6PR* resulted in a significant reduction of effector translocation compared with siOTP-NT–treated cells (Fig. 2*B*). Importantly, no toxic effects due to siRNA treatment were observed for all selected targets (*SI Appendix*, Fig. S1 *A* and *B*). These data reiterate the importance of a functional lysosomal environment for *C. burnetii* virulence.

The Role of Lysosomal Receptors LRP1 and M6PR during *C. burnetii* Infection. Given the integral role of receptors LRP1 and M6PR in lysosomal biogenesis (46) and the impact silencing expression of these receptors had on *C. burnetii* effector translocation (Fig. 2 *A* and *B*), further examination of *LRP1* and *M6PR* depletion was undertaken. Initially, the degradative capacity of lysosomes in siRNA-treated cells was determined using the DQ Green BSA reporter. The DQ-BSA (Dye Quenched-BSA) reporter is labeled with the fluorophore BODIPY FL, resulting in self-quenching of the dye. The molecule is endocytosed and accumulates in the lysosome, where proteases hydrolyze DQ Green BSA into smaller peptides, dequenching the dye and increasing fluorescence that can be detected using a fluorescence plate reader (47). The activity of lysosomal proteases is proportional to the rate of fluorescence increase. Individually silencing *LRP1* and *M6PR* demonstrated a trend toward decreased hydrolytic activity and silencing expression of both led to a significant reduction in the degradative capacity of the lysosome compared with siOTP-NT–treated cells (Fig. 2*C*). This decrease was not as severe as siRab7A-treated cells (in which lysosomal biogenesis is inhibited) or in siOTP-NT cells treated with the

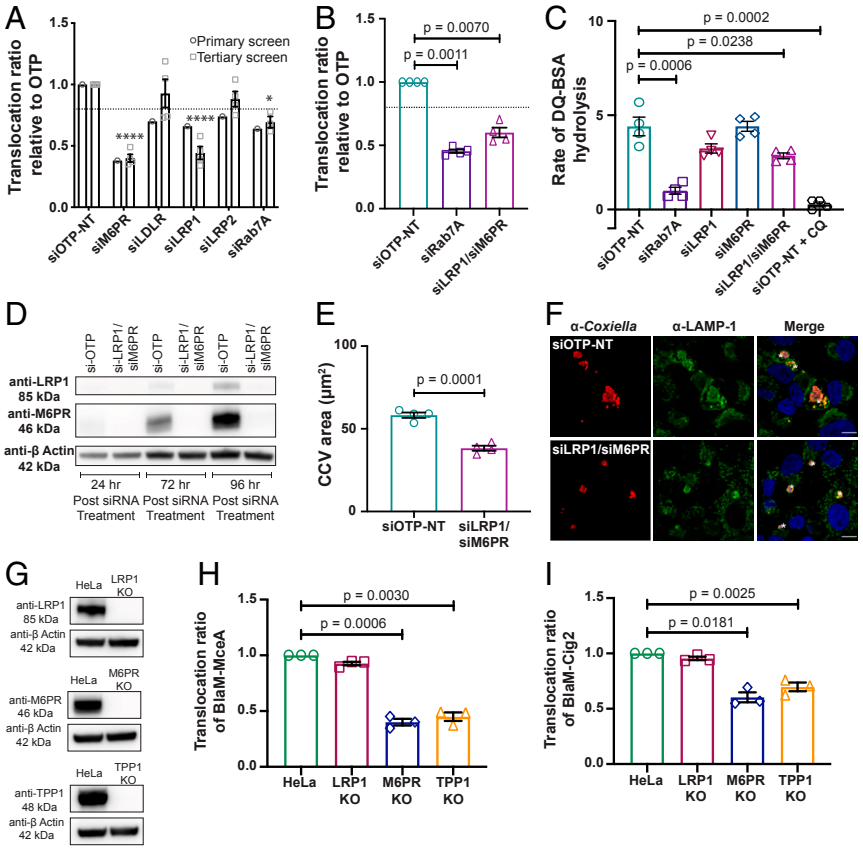

Fig. 2. Examination of the role of the lysosomal receptors LRP1 and M6PR and lysosomal protease TPP1 during *C. burnetii* infection. (*A* and *B*) Effector translocation was determined using CCF2-AM in HeLa cells infected with *C. burnetii* pBlaM–MceA following transfection with siRNA SMARTpools for 72 h. Results are expressed relative to the nontargeting control (siOTP-NT), with error bars indicating SEM from at least three independent experiments. Statistical difference between tested siRNA and siOTP-NT was determined using one-way ANOVA, followed by Dunnett's multiple-comparison posttest on raw data. $^{****}P = 0.0001$, $^{*}P < 0.05$. The dotted lines indicate a translocation ratio of 0.8 relative to siOTP-NT. The outcome from the automated primary screen (circle) is shown for comparison in *A*. (*C*) Lysosomal protease activity of HeLa cells transfected with siRNA SMARTpools for 72 h was determined using DQ Green BSA. Results are expressed as the average linear rate of DQ-BSA hydrolysis for each condition (12 wells in a 96-well plate) over 2 h from at least three independent experiments. Error bars denote SEM. Statistical difference between tested siRNA and siOTP-NT was determined using an unpaired, two-tailed *t* test on raw data. CQ, chloroquine. (*D*) Immunoblot analysis of cell lysates from HeLa cells treated with siRNA SMARTpools collected at 24, 72, and 96 h post siRNA treatment. The absence of protein expression in siRNA-treated cells compared with siOTP-NT–treated cells was confirmed using anti-LRP1 (*Top*) and anti-M6PR (*Middle*) antibodies. Anti–β-actin was used as a loading control (*Bottom*). (*E*) Intracellular replication of *C. burnetii* in HeLa cells treated with siRNA SMARTpools and subsequently infected with *C. burnetii* at an MOI of 50 for 3 d. Results are expressed as the average CCV area (μm^2) from four experiments with at least 50 CCVs measured per experiment. Error bars represent SEM. Statistical difference between siOTP-NT and tested siRNA was determined using an unpaired, two-tailed *t* test on raw data. (*F*) Representative confocal micrograph images of siRNA-treated HeLa cells infected for 3 d with *C. burnetii* used to quantify CCV area in *E*. Cells were stained with anti-*Coxiella* antibody (red), anti–LAMP-1 antibody (green), and DAPI (blue). (Scale bars, 10 μm.) Asterisks indicate CCV. (*G*) Immunoblot analysis of cell lysates from HeLa parent cells and LRP1 KO cells (*Top*), M6PR KO cells (*Middle*), and TPP1 KO cells (*Bottom*) illustrating the absence of protein expression in the KO cells using anti-LRP1, anti-M6PR, and anti-TPP1 antibodies, respectively. Anti–β-actin was used as a loading control. (*H* and *I*) Effector translocation was measured in KO cell lines infected with either *C. burnetii* pBlaM–MceA (*H*) or *C. burnetii* pBlaM–Cig2 (*I*). Results are expressed relative to HeLa cells, with error bars denoting SEM from three independent experiments. Statistical difference between HeLa and KO cell lines was determined using one-way ANOVA, followed by Dunnett's multiple-comparison posttest on raw data.

lysosomotropic agent chloroquine (Fig. 2*C*), suggesting that the degradative capacity of lysosomes in *LRP1*/*M6PR*-deficient cells is not completely abolished.

Since simultaneous depletion of both *LRP1* and *M6PR* significantly impacted the lysosomal degradative capacity of treated cells, the impact on *C. burnetii* virulence was investigated further. Western blot analysis confirmed almost complete abolishment of protein expression of both LRP1 and M6PR in siLRP1/siM6PR-treated cells (Fig. 2*D*). To eliminate a role for bacterial entry, differential intracellular/extracellular staining of *C. burnetii* was performed and no decrease in bacterial ingress was observed compared with siOTP-NT–treated cells (*SI Appendix*, Fig. S1*F*). Similarly, the capacity of *C. burnetii* to traffic through the host endocytic pathway to the lysosome-like compartment required for effector translocation may have been compromised. To assess this possibility, siRNA-treated HeLa cells were infected with *C. burnetii* for 6 h and the association of at least 150 internalized bacteria with the lysosomal marker LAMP-1 was quantified per experiment using fluorescence microscopy (*SI Appendix*, Fig. S1*H*). No difference in LAMP-1 association was observed during simultaneous silencing of *LRP1* and *M6PR*. To ascertain whether silencing *LRP1* and *M6PR* influenced *C. burnetii* replication, the CCV area was measured in siRNA-treated HeLa cells infected with *C. burnetii* for 3 d (Fig. 2*E*). Micrograph images (Fig. 2*F*) captured 3 d postinfection were used to determine the area of CCVs (Fig. 2*E*). Surprisingly, a significant reduction in CCV size was observed (mean CCV area, 38.25 ± 1.56 μm^2) in siLRP1/siM6PR-treated cells compared with siOTP-NT treatment (58.25 ± 1.62 μm^2) (Fig. 2*E*). This decrease did not translate to a defect in bacterial replication, quantified by measuring the *C.*

burnetii genome equivalents (*SI Appendix*, Fig. S1*J*). Collectively, these data suggest that while progression to the lysosome-like compartment and bacterial replication are not impacted during simultaneous silencing of *LRP1* and *M6PR*, expansion of the spacious replicative vacuole is significantly affected by the absence of both of these proteins. Importantly, analysis following a single siRNA treatment did not recapitulate this smaller CCV phenotype (*SI Appendix*, Fig. S1 *K* and *L*). This provides further evidence uncoupling the reduced translocation phenotype from CCV expansion, indicating that the overall degradative capacity of the CCV influences vacuole size independent of Dot/Icm efficiency.

The M6PR-Dependent Lysosomal Protease TPP1 Is Required for Efficient Dot/Icm Effector Translocation. Similar translocation defects were observed following depletion of LRP1, M6PR, or both receptors (Fig. 2 *A* and *B*), despite differential impact on overall lysosomal degradative capacity (Fig. 2*C*). This suggested that translocation efficiency is influenced by delivery and subsequent activity of specific lysosomal proteins rather than the overall lysosomal environment. Indeed, this hypothesis is supported by the genome-wide siRNA screen, where silencing expression of 39% of lysosomal proteins caused a significant drop in *C. burnetii* effector translocation (*SI Appendix*, Table S2). To further validate the role of individual lysosomal enzymes in effector translocation, the lysosomal serine protease TPP1 was also investigated.

TPP1 (tripeptidyl peptidase 1, also known as CLN2) is selectively transported to the lysosome by the lysosomal receptor M6PR (48), where it generates tripeptides from degraded proteins within the lysosome (49). The generation of HeLa cell lines completely devoid of either LRP1, M6PR, or TPP1 was pursued using the CRISPR-Cas9 genome-editing system. HeLa cells transfected with constructs that expressed guide RNA targeting *LRP1*, *M6PR*, or *TPP1* resulted in LRP1, M6PR, and TPP1 knockout (KO) cell lines with verified loss of each protein (Fig. 2*G*). Using the BlaM reporter fused to MceA, we observed a reduction in effector translocation in both M6PR and TPP1 KO cell lines of 60 and 55%, respectively, compared with the parent cell line (Fig. 2*H*). The LRP1 KO cell line did not reproduce the phenotype observed during siRNA treatment, indicating possible adaptation to loss of this receptor (Fig. 2*H*). To verify that the changes in translocation were not effector-specific, we also tested another known effector of the Dot/Icm secretion system (Cig2) (13), which produced similar results (40% reduction in M6PR KO and 30% reduction in TPP1 KO) (Fig. 2*I*).

Lysosomal Breakdown of Cellular Material Is Required for Effector Translocation and Virulence of *C. burnetii*. The siRNA screen indicated that gene silencing of several lysosomal proteases led to reduced effector translocation and the importance of this proteolysis was validated by the TPP1 KO cell line. This led to the hypothesis that protein degradation, and the subsequent products of this breakdown, may act as a signal to *C. burnetii* that the environment is appropriate for Dot/Icm activity. To test this hypothesis, effector translocation was examined following induction of autophagy to increase the amount of cellular material delivered to the lysosome. HeLa cells were infected with *C. burnetii* pBlaM–MceA for 20 h and then starved in Hank's balanced salt solution (HBSS) for 4 h or left untreated. Under starvation conditions, with increased autophagy, effector translocation was significantly increased ($P = 0.0067$) compared with untreated cells (Fig. 3*A*). This difference was abolished in the M6PR KO cell line (Fig. 3*A*). These data support the hypothesis that *C. burnetii* Dot/Icm effector translocation relies on delivery of the pathogen to a fully functional degradative compartment.

Expression of the Dot/Icm secretion apparatus genes as well as a subset of effector genes is regulated by the PmrA/B two-component system (20, 21). In other bacteria, the PmrB response regulator is activated by changes in pH or the concentration of Mg^{2+}, Fe^{3+}, or Al^{3+} cations (50). However, the activating signal for the *C. burnetii* PmrA/B two-component system has not been previously identified. In order to determine specific activators of PmrA/B-dependent gene expression, bacterial luciferase reporter strains (12, 21) were constructed using the strong constitutive promoter from *cbu0311* (12) and the PmrA-regulated *icmW* and *cig2* promoters (21). Light production from the *cbu0311*, *icmW*, and *cig2* promoters was measured in axenic *C. burnetii* cultures grown in complete ACCM-2 medium and then transferred into medium where the pH was adjusted or the medium composition had been altered as indicated (*SI Appendix*, Fig. S2). Modifications to pH resulted in similar changes among all promoters tested, indicating that transcriptional changes were not PmrA/B-specific. Similarly, no PmrA/B-dependent changes were observed with removal of specific components of ACCM-2, substitution with spent culture medium at various ratios, nor changes to cation concentration (*SI Appendix*, Fig. S2). This indicated that the lysosomal PmrB-activating signal was unlike that of related two-component systems.

Given the link between *C. burnetii* effector translocation and lysosomal protease activity (Figs. 2 *H* and *I* and 3*A*), a possible PmrA/B activation signal could be small peptides and/or amino acids within the lysosome. To investigate this, the same luciferase-expressing strains were grown axenically for 72 h and spiked with individual amino acids (10 mM diluted in H_2O) and light production was monitored at 0 min (to establish a baseline level) and 20 min postspike. Following normalization to *C. burnetii* P*311*-lux, a significant increase in light production was observed for *C. burnetii* P*icmW*-lux and *C. burnetii* P*cig2*-lux in the presence of cysteine and serine (Fig. 3*B*). Furthermore, an upward trend for many amino acids was observed, including alanine, aspartic acid, glutamic acid, glycine, phenylalanine, and proline (Fig. 3*B*). The addition of some of these amino acids to ACCM-2 further decreased the pH of this acidic medium. To eliminate this variable, the same experiments were performed using this subset of amino acids in Hepes buffer, which mitigated the substantial acidification of ACCM-2 after amino acid addition. The impact of several amino acids was diminished in Hepes buffer (*SI Appendix*, Fig. S2*F*), especially cysteine, glutamic acid, and glycine; however, a luciferase signal was still observed with the addition of phenylalanine and aspartic acid (*SI Appendix*, Fig. S2*F*). Given that addition of aspartic acid further acidified the media and also severely impacted the total light produced, additional experiments were performed in H_2O with the nonpolar amino acid phenylalanine to ensure signal transduction was not impacted by altered pH beyond physiological levels ($4.5 < pH > 8.0$) (51).

A small but statistically robust signal increase was observed in the presence of phenylalanine (Fig. 3*C*). Importantly, no increased luciferase signal was observed in the *C. burnetii pmrA*::Tn strain expressing the same luciferase reporters, indicating a direct link between phenylalanine and PmrA/B activation (Fig. 3*C*). A number of different amino acid combinations were attempted and the most consistent, PmrA-dependent response was observed by spiking media with phenylalanine, proline, and serine (Fig. 3*C*). Finally, the impact of these three amino acids in vivo was confirmed. Translocation of BlaM–MceA was measured in HeLa cells infected with *C. burnetii* pBlaM–MceA and simultaneously treated with either phenylalanine alone or in combination with proline and serine. An observable increase in effector translocation was detected in the presence of these amino acids when compared with H_2O alone (Fig. 3*D*). This critical experiment highlights that the characterization of the in vitro response to amino acids by *C. burnetii* translates to a physiologically relevant increase in effector translocation during infection.

RNA-Sequencing Analysis Reveals a Role for Amino Acids in Controlling the PmrA/B Regulon. To elucidate the impact of amino acids on gene regulation by the PmrA/B two-component system, transcriptional profiling was performed. The amino acid combination

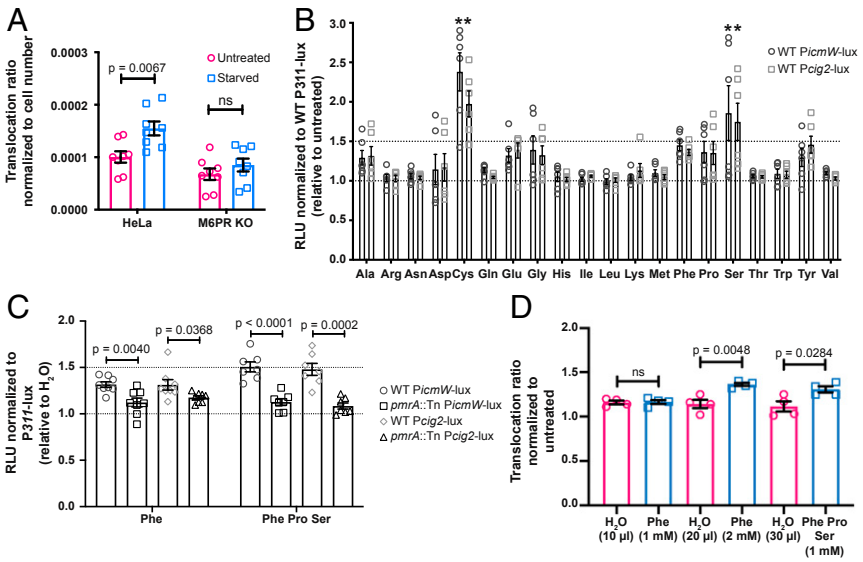

Fig. 3. Lysosomal breakdown of cellular material is required for effector translocation and virulence of *C. burnetii*. (*A*) HeLa parent and M6PR KO cell lines were starved in HBSS to induce autophagy, or left untreated for 4 h following 20 h infection with *C. burnetii* pBlaM–MceA. Results are presented as the average translocation ratio normalized to cell number, with error bars denoting SEM from eight independent experiments. Statistical difference between untreated and starved cells was determined using an unpaired, two-tailed *t* test. ns, not significant. (*B*) Axenic *C. burnetii* strains expressing a bacterial luciferase reporter under the control of a *C. burnetii* promoter (P*311*, P*icmW*, or P*cig2*) were grown for 72 h prior to the addition of different amino acids (10 mM) for 20 min. Data are presented as RLUs (relative light units) relative to untreated and normalized to P*311*-lux, with error bars representing SEM from six independent experiments. Statistical difference between P*311*-lux and P*icmW*-lux (circle) or P*cig2*-lux (square) was determined using two-way ANOVA, followed by Dunnett's multiple-comparison posttest. $*P < 0.0001$. (*C*) Axenic *C. burnetii* WT and *pmrA*::Tn strains expressing bacterial luciferase reporters were grown for 72 h prior to the addition of either phenylalanine alone (10 mM) or a combination of amino acids (10 mM each phenylalanine, proline, and serine) for 20 min. Data are presented as RLUs relative to addition of H_2O alone and normalized to the respective WT or *pmrA*::Tn P*311*-lux strains, with error bars representing SEM from at least six independent experiments. Statistical difference between WT P*icmW*-lux (circle) and *pmrA*::Tn P*icmW*-lux (square) or WT P*cig2*-lux (diamond) and *pmrA*::Tn P*cig2*-lux (triangle) was determined using an unpaired, two-tailed *t* test. (*D*) HeLa cells were infected with *C. burnetii* pBlaM–MceA and simultaneously treated with varying concentrations of amino acids or an equivalent volume of H_2O. Results are presented as the average translocation ratio normalized to untreated, with error bars denoting SEM from four independent experiments. Statistical difference between H_2O only and amino acid-treated cells was determined using an unpaired, two-tailed *t* test.

of phenylalanine, proline, and serine was selected since this combination demonstrated a robust PmrA-regulated response in the luciferase reporter strains (Fig. 3*C*) and the combination of these amino acids did not alter the pH of the media. The transcriptional profiles of *C. burnetii* wild type (WT) and *C. burnetii pmrA*::Tn, grown in axenic media for 3 d and spiked with either H_2O or the amino acid mixture for 20 min, were evaluated using RNA-sequencing (RNA-seq) (Datasets S4–S6). Comparison between the transcriptome of the water-treated samples and the RNA-seq analysis published by Beare et al. (21) revealed 62 common genes significantly up-regulated in *C. burnetii* WT compared with *C. burnetii pmrA*::Tn (*SI Appendix*, Table S3), suggesting that addition of water did not impact the PmrA/B transcriptional profile. Furthermore, this dataset identified an additional 36 genes as PmrA-regulated, of which 10 have previously been identified as Dot/Icm effectors (*SI Appendix*, Table S3). Of the 62 common genes, including genes encoding for components of the Dot/Icm secretion system and known effectors, the $\log_2$ fold change of *C. burnetii* WT H_2O compared with *C. burnetii pmrA*::Tn H_2O for this study is shown in Fig. 4*A*. To understand whether the presence of amino acids changed the transcriptional profile of these 62 genes, comparison between *C. burnetii* WT amino acids and *C. burnetii* WT H_2O was performed (Fig. 4*B*). Of the 62 genes, 42 genes (68%) were up-regulated in the presence of amino acids. Importantly, this up-regulation was not observed when comparing the water and amino acid treatment of *C. burnetii pmrA*::Tn (Fig. 4*B*). Collectively, these data demonstrate that the presence of phenylalanine, proline, and serine specifically induces expression of PmrA-regulated genes.

Discussion

Unlike other intracellular bacterial pathogens, *C. burnetii*, the causative agent of human Q fever, relies on the eukaryotic host to deliver it to a lysosomal environment. Once resident in this normally bactericidal compartment, the pathogen activates the Dot/Icm secretion system to remodel the organelle into a replication-permissive environment. This study reports the global identification of the human proteins that contribute to *C. burnetii* Dot/Icm effector translocation, uncovering important details regarding the initiation of *C. burnetii* virulence. Environmental adaptation, mediated by tight control of transcription, is central to the success of many bacterial pathogens. *C. burnetii* uses the PmrA/B two-component system to sense the degradative lysosomal environment and induce a transcriptional shift that mediates virulence. The outcome of transcriptional up-regulation of both the Dot/Icm apparatus and effector repertoire, once in the lysosome, is the formation of the replicative CCV which expands to occupy much of the host cell cytoplasm and support *C. burnetii* replication.

The siRNA screen performed here has exploited the lysosomal dependency of *C. burnetii* Dot/Icm activation to reveal many features of the host–pathogen interaction during establishment of *C. burnetii* infection. Human proteins that facilitate transport of microbes to the lysosome and proteins that create the degradative environment sensed by *C. burnetii* were identified in this screen. In addition, this screen also identified host factors that may be involved in *C. burnetii* invasion of HeLa cells. The *C. burnetii* outer-membrane protein OmpA has a role in facilitating *C. burnetii* entry of nonphagocytic cells; however, the host receptor for this invasin remains unknown (14). Likely candidates

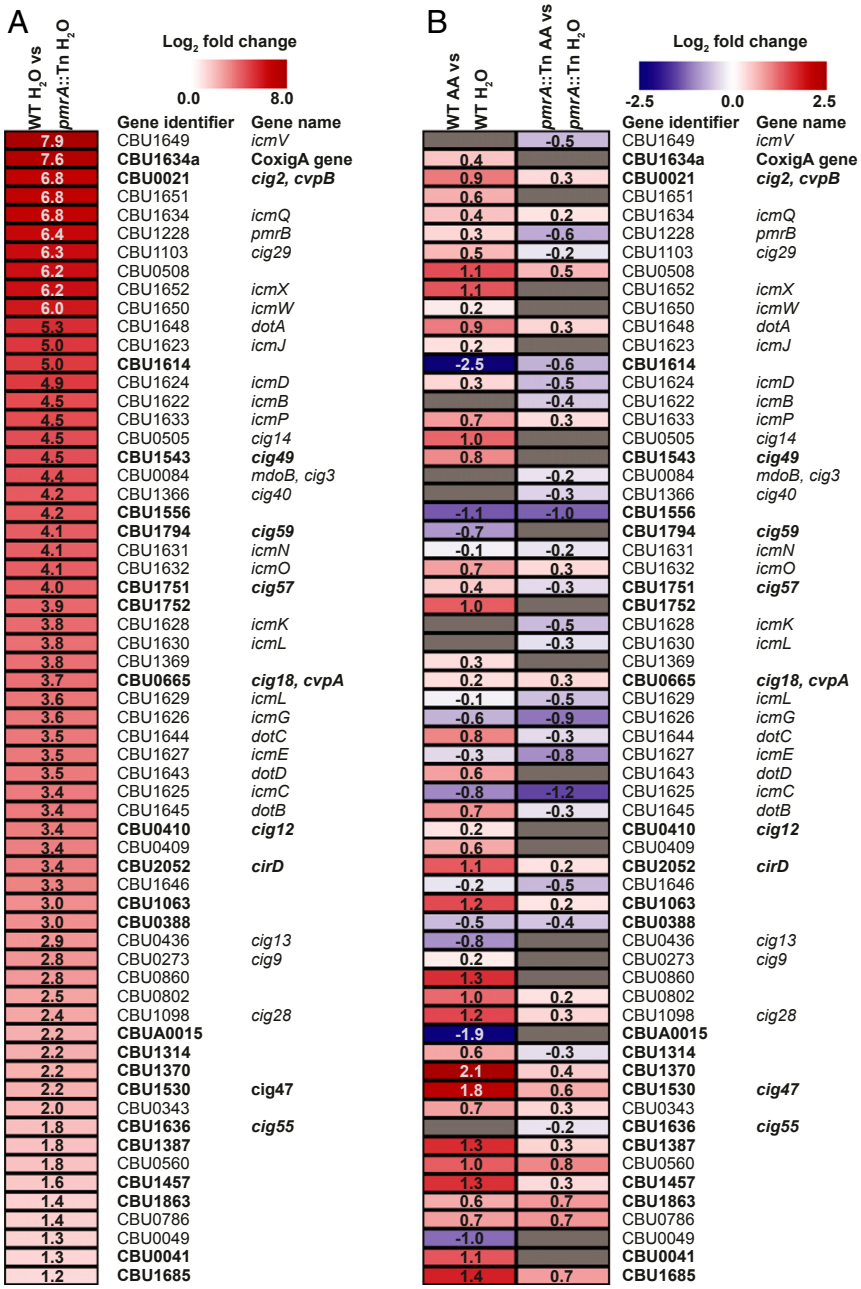

Fig. 4. RNA-seq analysis reveals a role for amino acids in controlling the PmrA/B regulon. (*A*) Heatmap of the comparison between *C. burnetii* WT H_2O and *pmrA*::Tn H_2O from this study of the 62 genes shown by both RNA-seq studies. Genes are ranked highest to lowest according to $\log_2$ fold change values (shown within). (*B*) Heatmaps representing the $\log_2$ fold change ($P_{adj} < 0.05$) of the 62 common genes after addition of the amino acid mixture composed of phenylalanine (10 mM), proline (10 mM), and serine (10 mM). Comparison between *C. burnetii* WT AA (amino acids) and *C. burnetii* WT H_2O is shown on the *Left* and comparison between *C. burnetii pmrA*::Tn AA and *C. burnetii pmrA*::Tn H_2O is displayed on the *Right*. The $\log_2$ fold change values are indicated within. Gray boxes represent genes with a $\log_2$ fold change ($P_{adj} > 0.05$). Experimentally verified effectors are indicated in bold. Data are also presented in Datasets S4–S6.

include integrin proteins; indeed, gene silencing of several alpha and beta integrins led to reduced effector translocation. Silencing integrin beta-8 (*ITGB8*) caused the most severe defect, with a 55% reduction in effector translocation. Similarly, gene silencing of either integrin alpha-2 or beta-1, which are known to form heterodimers in HeLa cells (52), demonstrated a 40% drop in effector translocation.

Transport of microbes through the endocytic pathway to the lysosome represents a fundamental innate immune process. The siRNA screen performed here provides validation and insight into the human proteins that are involved in this process. Adaptor proteins, Rab GTPases, coatomer components, SNAREs, and VPS proteins were all validated as contributing to *C. burnetii* Dot/Icm effector translocation, many presumably by contributing to delivery of the pathogen to the lysosome. Most interestingly, this siRNA screen demonstrated that many lysosomal proteins, including proteases such as TPP1, contribute to *C. burnetii* virulence. TMEM163, recently characterized as a lysosomal zinc transporter (53, 54), was validated as a high-confidence hit, with one of the most significant impacts on Dot/Icm effector translocation, likely

due to the importance of zinc as a cofactor for lysosomal enzymes. Similarly, M6PR, responsible for the delivery of many lysosomal proteins to the correct compartment, is also required for appropriate Dot/Icm effector translocation and efficient intracellular replication of *C. burnetii.* Overall, gene silencing 73 out of 185 known lysosomal proteins led to a reduction in Dot/Icm effector translocation. Given the overrepresentation of lysosomal proteins, the results from this screen may provide an opportunity to discover novel lysosomal proteins.

The requirement for specific lysosomal proteases, such as TPP1, for efficient Dot/Icm effector translocation led to the hypothesis that *C. burnetii* induces the activation of the Dot/Icm system in response to protein degradation in the lysosome. This was supported by demonstration that increased autophagy, and therefore increased delivery of protease substrate to the lysosome, causes increased Dot/Icm effector translocation in a manner that is dependent on M6PR. Importantly, analysis of the downstream progression of *C. burnetii* infection demonstrated that loss of these proteins, and subsequent reduced Dot/Icm translocation, does not necessarily impact CCV biogenesis and pathogen replication. This likely indicates that infection can progress as long as Dot/Icm effector translocation reaches a critical threshold level. It is plausible that this observation reflects the permissive nature of the host cell used in these studies. HeLa cells, with a less active lysosomal network, may still facilitate replication of *C. burnetii* with suboptimal levels of effector delivery. However, in the predominant natural host cell, alveolar macrophages, a more developed lysosomal compartment, would likely further promote effector delivery but perturbation of this compartment may have a more significant impact on infection progression.

A series of luciferase reporter strains has allowed us to demonstrate that the *C. burnetii* PmrA/PmrB two-component system responds to specific amino acids that are found at high concentration in the lysosome (55). The PmrA/PmrB two-component system has been well-characterized in both *L. pneumophila* and *C. burnetii* as controlling the expression of genes encoding for structural components of the Dot/Icm apparatus and a large subset of Dot/Icm effectors (13, 20, 21, 56, 57). Given this transcriptional influence, it is not surprising that this two-component system is required for intracellular growth of both pathogens (13, 20, 21). The PmrB sensor histidine kinases of *L. pneumophila* and *C. burnetii* share 50% identity across the entire protein and are highly conserved within the histidine kinase domain. Importantly, the predicted extracellular component of PmrB that recognizes environmental signals is the least conserved region, supporting the hypothesis that these proteins respond to different extracellular stimuli.

Homologous PmrA/PmrB two-component systems have been well-characterized in a range of bacterial species and have been shown to contribute to virulence of several pathogens including *Salmonella enterica* serovar Typhimurium and *Pseudomonas aeruginosa* (reviewed in ref. 50). In these bacteria, environmental stimuli such as low Mg^{2+} or high Fe^{3+} are recognized by PmrB, leading to activation of the response regulator PmrA and transcriptional changes that promote LPS alterations to facilitate resistance to antibiotics such as polymyxin B and to toxic metals such as Fe^{3+} (58, 59).

Initial characterization of the *C. burnetii* luciferase reporters used here demonstrated that the *C. burnetii* PmrA/PmrB system does not respond to these stimuli. Rather, we have demonstrated that *C. burnetii* PmrB can sense amino acids, particularly phenylalanine, proline, and serine, to induce activation of PmrA. The recent first comprehensive analysis of metabolites in the lysosome demonstrates the presence of these amino acids used here to induce a PmrA-dependent transcriptional response (55). Characterization of the lysosome metabolome has also demonstrated that the oxidized form of cysteine, cystine, represents a defining characteristic of the lysosome, with a 28-fold higher concentration in the lysosome compared with the rest of the human cell (55). Abu-Remaileh et al. (55) also demonstrated that vATPase inhibition leads to a significant decrease in lysosomal cystine, supporting our previous observations that low lysosomal pH is required for *C. burnetii* Dot/Icm function (18). Interestingly, our data indicate that Dot/Icm function may also be inhibited by unusually high concentrations of particular amino acids as the siRNA screen demonstrated an effector translocation defect for several amino acid transporters including cystinosin, the lysosomal cystine transporter (CTNS) which exports cystine to the cytosol.

Sensing and responding to amino acids is not restricted to *C. burnetii*. The recently characterized GluR-GluK two-component system of *Streptomyces coelicolor* responds to extracellular glutamate to increase expression of a glutamate uptake system (60). This response allows a transcriptional shift that can impact metabolic activity in response to nutrient availability. In contrast, the PmrA/B response of *C. burnetii* is not linked to metabolic changes but to transition to a virulent phenotype. Transcriptional virulence induction in response to amino acids also appears true for enterohemorrhagic *Escherichia coli* (EHEC) as a recent report indicated that exogenous cysteine can be sensed by the EHEC cysteine utilization regulator CutR, leading to increased expression of genes within the virulence-associated locus of the enterocyte effacement pathogenicity island (61).

Specific two-component systems can respond to more than one stimulus (50, 62). Thus, further investigation may demonstrate that other lysosomal breakdown products also stimulate *C. burnetii* PmrA/PmrB activity, particularly given that silencing of MANBA and lysosomal sialidase (NEU1) both reduced *C. burnetii* Dot/Icm effector translocation. This study has significantly broadened our understanding of *C. burnetii* pathogenesis and the intimate relationships between intracellular bacterial virulence and their subcellular niche.

Materials and Methods

Data Availability Statement. The complete siRNA screen data is available in Dataset S1. All RNA-seq data is available in Datasets S4–S6.

Cell Culture. HeLa cells were maintained in Dulbecco's modified Eagle's medium (GlutaMAX; Gibco) supplemented with 10% heat-inactivated FBS at 37 °C in 5% CO_2.

Bacterial Strains. *C. burnetii* Nine Mile phase II (RSA439, clone 4) strains were cultured axenically in ACCM-2 at 37 °C in 5% CO_2 and 2.5% O_2 (63). Chloramphenicol and kanamycin were added to ACCM-2 at 3 and 350 μg/mL, respectively, when required. *E. coli* DH5α, *E. coli* PIR1, or *E. coli* PIR2 strains were grown in Luria-Bertani (LB) broth or on LB agar plates containing ampicillin (100 μg/mL), chloramphenicol (12.5 μg/mL), or kanamycin (100 μg/mL) as necessary.

High-Throughput siRNA Screening. HeLa cells (3,920 cells per well) were reverse-transfected in black-walled clear-bottom 96-well plates (Corning) with siGENOME SMARTpool siRNAs (final concentration 40 nM) using DharmaFECT 1 lipid transfection reagent (0.1 μL per well) (Dharmacon RNAi Technologies). Genome-wide siRNA libraries (catalog numbers in Dataset S1) were screened at the Victorian Centre for Functional Genomics at the Peter MacCallum Cancer Centre. Each well in the siGENOME SMARTpool siRNA library contained 4 siRNAs targeting different sequences of the target transcript. A deconvolution validation screen was performed using the individual siRNA duplexes, all four on the same library plate (catalog numbers in Dataset S2) at 25 nM with the same assay conditions as above.

Cells were reverse-transfected using the SciClone ALH3000 lab automation liquid handler (Caliper Life Sciences) and EL406 microplate washer dispenser (BioTek). Cells were transfected in duplicate and media were changed 24 h after transfection using the EL406 microplane washer dispenser (BioTek). Seventy-two hours posttransfection, cells were infected with *C. burnetii* pBlaM–MceA at a multiplicity of infection (MOI) of 300 for 24 h. Infected cells were loaded with CCF2-AM using the LiveBLAzer FRET B/G Loading Kit (Invitrogen) and 0.1 M probenecid. The CLARIOstar microplate reader (BMG LABTECH) was used to quantify translocation. The ratio of 450 nm (blue; product in Dataset S1) to 520 nm (green; substrate in Dataset S1) was

calculated. Cell viability was determined by fixing (4% paraformaldehyde for 15 min) and staining cells with DRAQ5 fluorescent probe solution (Thermo Scientific; 1:4,000 in PBS). A CellInsight High-Content Screening microscope (Thermo Scientific) was used to quantify the number of nuclei per well for nine fields using a 5× objective alongside the Target Activation bioapplication of HCS Studio cell analysis software (iDev workflow). Details of the bioinformatic analysis of siRNA screen data are described in *SI Appendix, Materials and Methods*.

Generation of CRISPR Cell Lines. CRISPR-Cas9 genome editing was performed using pX459 v2.0, a gift from Feng Zhang (Addgene plasmid 62988). Guide RNA specific for *LRP1* (64), *M6PR*, and *TPP1* (designed using https://zlab.bio/guide-design-resources; *SI Appendix*, Table S4) was cloned into pX459 (65). HeLa cells were seeded at 3.75×10^5 per well in six-well tissue-culture plates and cotransfected using Lipofectamine 3000 and a total of 2,500 ng DNA specific to either one exon (*LRP1*) or two exons (*M6PR* and *TPP1*). Cells were selected with puromycin (2.5 μg/mL) and clonally isolated in 96-well tissue-culture plates.

Generation of Luciferase-Expressing *C. burnetii* Strains. Integration plasmids [pMiniTn7T-Kan and pMiniTn7T-CAT::*luxCDABE* (21)] were a gift from P. Beare (Rocky Mountain Laboratories, NIH, Hamilton, MT). The *luxCDABE* operon, T0T1 terminator, and promoters amplified from *C. burnetii* genomic DNA were added to pMiniTn7T as described in *SI Appendix*, Table S4. The integration of the luciferase-expressing plasmids into *C. burnetii* WT and *C. burnetii pmrA*::Tn was achieved by electroporation and selection as described previously (10, 66). Luciferase-expressing *C. burnetii* were analyzed for a response to pH or altered medium composition as described in *SI Appendix, Materials and Methods*.

Amino Acid Analysis. The 20 essential amino acids were diluted in either dH_2O or 1 M Hepes buffer to a final concentration of 100 mM. Axenically grown *C. burnetii* strains were added to white-bottomed 96-well tissue-culture plates at 1×10^5 GE (genome equivalent) per well and incubated at 37 °C with 5% CO_2 and 2.5% O_2 for 72 h. Amino acids were added at a final concentration of 10 mM (or equal volume of carrier) to individual wells in duplicate. The plates were then incubated at 37 °C for 20 min using the CLARIOstar microplate reader in which light production was measured at 0 min (to provide a baseline measurement) and 20 min after the addition of amino acids. Light production values of P*icmW* and P*cig2* strains were adjusted relative to P*311* following normalization to carrier-treated samples.

DQ-BSA Assay. DQ Green BSA (Life Technologies) was used to measure lysosomal protease activity in cells as described previously (67), with slight modifications described in *SI Appendix, Materials and Methods*.

RNA-Seq Analysis. *C. burnetii* WT and *C. burnetii pmrA*::Tn were grown axenically for 7 d in quadruplicate and subsequently inoculated in duplicate into 30 mL ACCM-2 at a concentration of 1×10^6 GE per mL. Bacteria were grown in ACCM-2 for 72 h, after which each strain was treated with either dH_2O or an amino acid mixture consisting of 10 mM phenylalanine, 10 mM proline, and 10 mM serine and incubated at 37 °C in 5% CO_2 and 2.5% O_2 for a further 20 min. Cultures were harvested at 3,250 × *g* for 15 min at 4 °C and RNA was extracted using TRIsure (Bioline) according to the manufacturer's instructions. Samples were treated for DNA contamination using an RNase-Free DNase Set (QIAGEN) and cleaned using the RNease Mini Kit (QIAGEN) as per the manufacturer's instructions.

High-quality RNA samples, as assessed on an Agilent 2100 Bioanalyzer, were submitted to the Australian Genome Research Facility for ribosomal RNA depletion using Ribo-Zero bacteria (Illumina) and high-throughput 100-bp single-end sequencing on the Illumina HiSeq 2500. Transcripts were analyzed as described in *SI Appendix, Materials and Methods*.

Please refer to *SI Appendix, Materials and Methods* for more information regarding siRNA transfections, translocation assays, real-time quantification, Western blot analysis, *C. burnetii* infections, immunofluorescence staining, microscopy, and statistical analysis.

ACKNOWLEDGMENTS. Confocal microscopy was performed at the Biological Optical Microscopy Platform, The University of Melbourne (https://microscopy.unimelb.edu.au/). We thank Dan Thomas and Jennii Luu from the Victorian Centre for Functional Genomics for expert technical help during the screen. We acknowledge use of the services and facilities of the Australian Genome Research Facility. Single-copy integration plasmids were a gift from P. A. Beare and R. A. Heinzen, Rocky Mountain Laboratories, NIH. This research was supported by Australian National Health and Medical Research Council APP1063646 and APP1120344. The Victorian Centre for Functional Genomics (K.J.S.) is funded by the Australian Cancer Research Foundation, the Australian Phenomics Network through funding from the Australian Government's National Collaborative Research Infrastructure Strategy Program, and the Peter MacCallum Cancer Centre Foundation. L.E.E.-M. is funded by the Grimwade Fellowship from the Russell and Mab Grimwade Miegunyah Fund at The University of Melbourne and a Discovery Early Career Researcher Award Fellowship from the Australian Research Council (DE180100418).

1. C. Eldin *et al*., From Q fever to *Coxiella burnetii* infection: A paradigm change. *Clin. Microbiol. Rev.* **30**, 115–190 (2017).
2. M. Calverley, S. Erickson, A. J. Read, A. G. Harmsen, Resident alveolar macrophages are susceptible to and permissive of *Coxiella burnetii* infection. *PLoS One* **7**, e51941 (2012).
3. J. G. Graham *et al*., Virulent *Coxiella burnetii* pathotypes productively infect primary human alveolar macrophages. *Cell. Microbiol.* **15**, 1012–1025 (2013).
4. S. A. Coleman, E. R. Fischer, D. Howe, D. J. Mead, R. A. Heinzen, Temporal analysis of *Coxiella burnetii* morphological differentiation. *J. Bacteriol.* **186**, 7344–7352 (2004).
5. A. Lührmann, H. J. Newton, M. Bonazzi, Beginning to understand the role of the type IV secretion system effector proteins in *Coxiella burnetii* pathogenesis. *Curr. Top. Microbiol. Immunol.* **413**, 243–268 (2017).
6. A. Friedrich, J. Pechstein, C. Berens, A. Lührmann, Modulation of host cell apoptotic pathways by intracellular pathogens. *Curr. Opin. Microbiol.* **35**, 88–99 (2017).
7. A. Omsland *et al*., Host cell-free growth of the Q fever bacterium *Coxiella burnetii*. *Proc. Natl. Acad. Sci. U.S.A.* **106**, 4430–4434 (2009).
8. P. A. Beare, Genetic manipulation of *Coxiella burnetii*. *Adv. Exp. Med. Biol.* **984**, 249–271 (2012).
9. J. H. Moffatt, P. Newton, H. J. Newton, *Coxiella burnetii*: Turning hostility into a home. *Cell. Microbiol.* **17**, 621–631 (2015).
10. K. L. Carey, H. J. Newton, A. Lührmann, C. R. Roy, The *Coxiella burnetii* Dot/Icm system delivers a unique repertoire of type IV effectors into host cells and is required for intracellular replication. *PLoS Pathog.* **7**, e1002056 (2011).
11. P. A. Beare *et al*., Dot/Icm type IVB secretion system requirements for *Coxiella burnetii* growth in human macrophages. *MBio* **2**, e00175-11 (2011).
12. P. A. Beare, C. L. Larson, S. D. Gilk, R. A. Heinzen, Two systems for targeted gene deletion in *Coxiella burnetii*. *Appl. Environ. Microbiol.* **78**, 4580–4589 (2012).
13. H. J. Newton *et al*., A screen of *Coxiella burnetii* mutants reveals important roles for Dot/Icm effectors and host autophagy in vacuole biogenesis. *PLoS Pathog.* **10**, e1004286 (2014).
14. E. Martinez, F. Cantet, L. Fava, I. Norville, M. Bonazzi, Identification of OmpA, a *Coxiella burnetii* protein involved in host cell invasion, by multi-phenotypic high-content screening. *PLoS Pathog.* **10**, e1004013 (2014).
15. J. Qiu, Z. Q. Luo, Effector translocation by the *Legionella* Dot/Icm type IV secretion system. *Curr. Top. Microbiol. Immunol.* **376**, 103–115 (2013).
16. J. C. Kagan, C. R. Roy, *Legionella* phagosomes intercept vesicular traffic from endoplasmic reticulum exit sites. *Nat. Cell Biol.* **4**, 945–954 (2002).
17. H. Nagai *et al*., A C-terminal translocation signal required for Dot/Icm-dependent delivery of the *Legionella* RalF protein to host cells. *Proc. Natl. Acad. Sci. U.S.A.* **102**, 826–831 (2005).
18. H. J. Newton, J. A. McDonough, C. R. Roy, Effector protein translocation by the *Coxiella burnetii* Dot/Icm type IV secretion system requires endocytic maturation of the pathogen-occupied vacuole. *PLoS One* **8**, e54566 (2013).
19. P. Newton, E. A. Latomanski, H. J. Newton, Applying fluorescence resonance energy transfer (FRET) to examine effector translocation efficiency by *Coxiella burnetii* during siRNA silencing. *J. Vis. Exp.* (113), e54210 (2016).
20. T. Zusman *et al*., The response regulator PmrA is a major regulator of the *icm/dot* type IV secretion system in *Legionella pneumophila* and *Coxiella burnetii*. *Mol. Microbiol.* **63**, 1508–1523 (2007).
21. P. A. Beare *et al*., Essential role for the response regulator PmrA in *Coxiella burnetii* type 4B secretion and colonization of mammalian host cells. *J. Bacteriol.* **196**, 1925–1940 (2014).
22. J. A. McDonough *et al*., Host pathways important for *Coxiella burnetii* infection revealed by genome-wide RNA interference screening. *MBio* **4**, e00606-12 (2013).
23. L. F. Fielden *et al*., A farnesylated *Coxiella burnetii* effector forms a multimeric complex at the mitochondrial outer membrane during infection. *Infect. Immun.* **85**, e01046-16 (2017).
24. P. Baum *et al*., Off-target analysis of control siRNA molecules reveals important differences in the cytokine profile and inflammation response of human fibroblasts. *Oligonucleotides* **20**, 17–26 (2010).
25. X. Liu, R. L. Erikson, Polo-like kinase (Plk)1 depletion induces apoptosis in cancer cells. *Proc. Natl. Acad. Sci. U.S.A.* **100**, 5789–5794 (2003).
26. A. Birmingham *et al*., Statistical methods for analysis of high-throughput RNA interference screens. *Nat. Methods* **6**, 569–575 (2009).
27. X. D. Zhang *et al*., Robust statistical methods for hit selection in RNA interference high-throughput screening experiments. *Pharmacogenomics* **7**, 299–309 (2006).
28. P. D. Thomas *et al*., PANTHER: A browsable database of gene products organized by biological function, using curated protein family and subfamily classification. *Nucleic Acids Res.* **31**, 334–341 (2003).

29. C. C. Farnsworth, M. C. Seabra, L. H. Ericsson, M. H. Gelb, J. A. Glomset, Rab geranylgeranyl transferase catalyzes the geranylgeranylation of adjacent cysteines in the small GTPases Rab1A, Rab3A, and Rab5A. *Proc. Natl. Acad. Sci. U.S.A.* **91**, 11963–11967 (1994).
30. Y. Zhen, H. Stenmark, Cellular functions of Rab GTPases at a glance. *J. Cell Sci.* **128**, 3171–3176 (2015).
31. J. K. Ryu, R. Jahn, T. Y. Yoon, Review: Progresses in understanding *N*-ethylmaleimide sensitive factor (NSF) mediated disassembly of SNARE complexes. *Biopolymers* **105**, 518–531 (2016).
32. D. O. Clary, I. C. Griff, J. E. Rothman, SNAPs, a family of NSF attachment proteins involved in intracellular membrane fusion in animals and yeast. *Cell* **61**, 709–721 (1990).
33. V. Malhotra, L. Orci, B. S. Glick, M. R. Block, J. E. Rothman, Role of an *N*-ethylmaleimide-sensitive transport component in promoting fusion of transport vesicles with cisternae of the Golgi stack. *Cell* **54**, 221–227 (1988).
34. M. Gallon, P. J. Cullen, Retromer and sorting nexins in endosomal sorting. *Biochem. Soc. Trans.* **43**, 33–47 (2015).
35. M. N. Seaman, J. M. McCaffery, S. D. Emr, A membrane coat complex essential for endosome-to-Golgi retrograde transport in yeast. *J. Cell Biol.* **142**, 665–681 (1998).
36. M. Babst, D. J. Katzmann, W. B. Snyder, B. Wendland, S. D. Emr, Endosome-associated complex, ESCRT-II, recruits transport machinery for protein sorting at the multivesicular body. *Dev. Cell* **3**, 283–289 (2002).
37. M. Babst, B. Wendland, E. J. Estepa, S. D. Emr, The Vps4p AAA ATPase regulates membrane association of a Vps protein complex required for normal endosome function. *EMBO J.* **17**, 2982–2993 (1998).
38. M. G. Gutierrez *et al*., Autophagy induction favours the generation and maturation of the *Coxiella*-replicative vacuoles. *Cell. Microbiol.* **7**, 981–993 (2005).
39. E. A. Latomanski, H. J. Newton, Interaction between autophagic vesicles and the *Coxiella*-containing vacuole requires CLTC (clathrin heavy chain). *Autophagy* **14**, 1710–1725 (2018).
40. R. Khandia *et al*., A comprehensive review of autophagy and its various roles in infectious, non-infectious, and lifestyle diseases: Current knowledge and prospects for disease prevention, novel drug design, and therapy. *Cells* **8**, E674 (2019).
41. D. Howe, J. G. Shannon, S. Winfree, D. W. Dorward, R. A. Heinzen, *Coxiella burnetii* phase I and II variants replicate with similar kinetics in degradative phagolysosome-like compartments of human macrophages. *Infect. Immun.* **78**, 3465–3474 (2010).
42. M. Maurin, A. M. Benoliel, P. Bongrand, D. Raoult, Phagolysosomes of *Coxiella burnetii*-infected cell lines maintain an acidic pH during persistent infection. *Infect. Immun.* **60**, 5013–5016 (1992).
43. M. Thelen, D. Winter, T. Braulke, V. Gieselmann, SILAC-based comparative proteomic analysis of lysosomes from mammalian cells using LC-MS/MS. *Methods Mol. Biol.* **1594**, 1–18 (2017).
44. S. Kissing, P. Saftig, A. Haas, Vacuolar ATPase in phago(lyso)some biology. *Int. J. Med. Microbiol.* **308**, 58–67 (2018).
45. T. Braulke, J. S. Bonifacino, Sorting of lysosomal proteins. *Biochim. Biophys. Acta* **1793**, 605–614 (2009).
46. C. Staudt, E. Puissant, M. Boonen, Subcellular trafficking of mammalian lysosomal proteins: An extended view. *Int. J. Mol. Sci.* **18**, E47 (2016).
47. R. Marwaha, M. Sharma, DQ-Red BSA trafficking assay in cultured cells to assess cargo delivery to lysosomes. *Bio Protoc.* **7**, e2571 (2017).
48. M. Qian, D. E. Sleat, H. Zheng, D. Moore, P. Lobel, Proteomics analysis of serum from mutant mice reveals lysosomal proteins selectively transported by each of the two mannose 6-phosphate receptors. *Mol. Cell. Proteomics* **7**, 58–70 (2008).
49. D. J. Vines, M. J. Warburton, Classical late infantile neuronal ceroid lipofuscinosis fibroblasts are deficient in lysosomal tripeptidyl peptidase I. *FEBS Lett.* **443**, 131–135 (1999).
50. H. D. Chen, E. A. Groisman, The biology of the PmrA/PmrB two-component system: The major regulator of lipopolysaccharide modifications. *Annu. Rev. Microbiol.* **67**, 83–112 (2013).
51. A. Asokan, M. J. Cho, Exploitation of intracellular pH gradients in the cellular delivery of macromolecules. *J. Pharm. Sci.* **91**, 903–913 (2002).
52. T. Riikonen, P. Vihinen, M. Potila, W. Rettig, J. Heino, Antibody against human alpha 1 beta 1 integrin inhibits HeLa cell adhesion to laminin and to type I, IV, and V collagens. *Biochem. Biophys. Res. Commun.* **209**, 205–212 (1995).
53. M. P. Cuajungco, K. Kiselyov, The mucolipin-1 (TRPML1) ion channel, transmembrane-163 (TMEM163) protein, and lysosomal zinc handling. *Front. Biosci.* **22**, 1330–1343 (2017).
54. M. P. Cuajungco *et al*., Cellular zinc levels are modulated by TRPML1-TMEM163 interaction. *Traffic* **15**, 1247–1265 (2014).
55. M. Abu-Remaileh *et al*., Lysosomal metabolomics reveals V-ATPase- and mTOR-dependent regulation of amino acid efflux from lysosomes. *Science* **358**, 807–813 (2017).
56. S. Al-Khodor, S. Kalachikov, I. Morozova, C. T. Price, Y. Abu Kwaik, The PmrA/PmrB two-component system of *Legionella pneumophila* is a global regulator required for intracellular replication within macrophages and protozoa. *Infect. Immun.* **77**, 374–386 (2009).
57. G. Segal, The *Legionella pneumophila* two-component regulatory systems that participate in the regulation of Icm/Dot effectors. *Curr. Top. Microbiol. Immunol.* **376**, 35–52 (2013).
58. M. M. Wösten, L. F. Kox, S. Chamnongpol, F. C. Soncini, E. A. Groisman, A signal transduction system that responds to extracellular iron. *Cell* **103**, 113–125 (2000).
59. J. C. Perez, E. A. Groisman, Acid pH activation of the PmrA/PmrB two-component regulatory system of *Salmonella enterica*. *Mol. Microbiol.* **63**, 283–293 (2007).
60. L. Li, W. Jiang, Y. Lu, A novel two-component system, GluR-GluK, involved in glutamate sensing and uptake in *Streptomyces coelicolor*. *J. Bacteriol.* **199**, e00097-17 (2017).
61. R. Pifer, R. M. Russell, A. Kumar, M. M. Curtis, V. Sperandio, Redox, amino acid, and fatty acid metabolism intersect with bacterial virulence in the gut. *Proc. Natl. Acad. Sci. U.S.A.* **115**, E10712–E10719 (2018).
62. K. M. Carlson-Banning, V. Sperandio, Enterohemorrhagic *Escherichia coli* outwits hosts through sensing small molecules. *Curr. Opin. Microbiol.* **41**, 83–88 (2018).
63. A. Omsland *et al*., Isolation from animal tissue and genetic transformation of *Coxiella burnetii* are facilitated by an improved axenic growth medium. *Appl. Environ. Microbiol.* **77**, 3720–3725 (2011).
64. L. Luo *et al*., TLR crosstalk activates LRP1 to recruit Rab8a and PI3Kγ for suppression of inflammatory responses. *Cell Rep.* **24**, 3033–3044 (2018).
65. F. A. Ran *et al*., Genome engineering using the CRISPR-Cas9 system. *Nat. Protoc.* **8**, 2281–2308 (2013).
66. P. A. Beare, K. M. Sandoz, A. Omsland, D. D. Rockey, R. A. Heinzen, Advances in genetic manipulation of obligate intracellular bacterial pathogens. *Front. Microbiol.* **2**, 97 (2011).
67. L. Fernandez-Mosquera *et al*., Mitochondrial respiratory chain deficiency inhibits lysosomal hydrolysis. *Autophagy* **15**, 1572–1591 (2019).